Surface & Coatings Technology 202 (2008) 5158–5161

Contents lists available at ScienceDirect

Surface & Coatings Technology

journal homepage: www.elsevier.com/locate/surfcoat

The influence of age-hardening on turning and milling performance of Ti–Al–N coated inserts

Li Chen [a,b,*], Yong Du [a], Paul H. Mayrhofer [b], She Q. Wang [a,c], Jia Li [c]

[a] State Key Laboratory of Powder Metallurgy, Central South University, Changsha Hunan, 410083, China
[b] Department of Physical Metallurgy and Materials Testing, Montanuniversität Leoben, Leoben, 8700, Austria
[c] Zhuzhou Cemented Carbide Cutting Tools Co., LTD, Zhuzhou, 412007, China

ARTICLE INFO

Article history:
Received 10 March 2008
Accepted in revised form 22 May 2008
Available online 29 May 2008

Keywords:
(Ti,Al)N
Age hardening
Machining

ABSTRACT

Ti–Al–N coatings are well known for their excellent properties and age-hardening abilities. Here we show that the life-time of coated inserts during turning of stainless steel can be increased to 200% by post-deposition vacuum annealing at 900 °C combined with a ~1 K/min vacuum furnace cooling. During milling of 42CrMo steel an increase in tool life-time to 140% is only obtained if the cooling condition after annealing at 900 °C contains a fast segment with 50 K/min from 800 to 700 °C. Thereby, the Co-binder in cemented carbide exhibits a retarded phase transformation from cubic to hexagonal. Consequently, the fracture toughness of the cemented carbide is reduced only from ~10.8 to 10.4 MPa√m while the coating still has an adhesive strength of ~65 N.

Our results indicate that best machining performances of coated inserts are obtained after annealing at 900 °C where the supersaturated $Ti_{0.34}Al_{0.66}N$ coating undergoes spinodal decomposition to form nm-sized cubic TiN and AlN domains resulting in a hardness increase from 34.5 to 38.7 GPa. Additionally, we demonstrate that careful attention needs to be paid on the influence of annealing conditions on adhesive strength and fracture toughness of coated inserts.

© 2008 Elsevier B.V. All rights reserved.

1. Introduction

Ti–Al–N coatings have received widespread attention especially for machining applications due to their excellent tribological properties, high temperature oxidation resistance, and high chemical stability [1,2]. Improvement of their properties can be obtained by an optimized Al content, microstructure (e.g., changing from single layer to multi-layer and superlattice) and crystal orientation [3–5]. In addition, the microstructure evolution of Ti–Al–N coatings during annealing has attracted attention due to the observed age-hardening abilities [6–8]. Age-hardening is well described and investigated for bulk materials like Al-based alloys and steels since the early work of Cahn [9]. During annealing above 600 °C, supersaturated Ti–Al–N coatings prepared by plasma assisted physical vapour deposition (PVD) decompose to form cubic (c) TiN and c-AlN domains [6,8,10]. The formation of nm-sized cubic TiN and AlN domains within the remaining cubic Ti–Al–N matrix causes an increase in hardness. The latter plays an essential role in industrial application in combination with the oxidation resistance. These are major considerations for the improvement of machining performances of hard coatings in general [6,10]. Furthermore, it is reported that the cutting performance of coated tools can be improved through annealing as thereby the internal stresses of the coatings decrease [11,12]. Nevertheless, there is only limited information on the industrial application of age-hardened coatings.

For $Ti_{0.33}Al_{0.67}N$ coatings, an improvement during continuous cutting of 1040 steel is obtained by a post-deposition annealing at 700 and 900 °C [13,14]. Contrary to that, the milling performance of 4340 and H13 steel is reduced when the coated inserts are annealed above 700 °C [14]. Milling demands a high toughness in addition to sharpness of the cutting tool edge as the tool repeatedly enters, cuts, and leaves the workpiece, sustaining both mechanical and thermal shocks. In addition, it is important to consider differences in thermal expansion between coating and substrate. Rapid cooling gives rise to crack-formation in the coating and decreases its adhesion to the substrate. The fracture toughness of cemented carbide is reduced by slow cooling due to transformation of the Co binder from face centered cubic (c) to hexagonal close packed (h) in the temperature range 800–700 °C [15]. Thus, the cooling condition after the annealing treatment of Ti–Al–N coated cemented carbide tools is essential for optimized performances.

The purpose of this work is to investigate the effect of annealing on the machining properties of Ti–Al–N coated inserts. Consequently, we investigate the microstructure, hardness, and adhesion of Ti–Al–N coatings in combination to fracture toughness measurements of the cemented carbide substrate as a function of annealing temperature

* Corresponding author. Department of Physical Metallurgy and Materials Testing, Montanuniversität Leoben, Leoben, 8700, Austria. Tel.: +43 3842 4024236; fax: +43 3842 4024202.
E-mail address: chenli_927@126.com (L. Chen).

0257-8972/$ – see front matter © 2008 Elsevier B.V. All rights reserved.
doi:10.1016/j.surfcoat.2008.05.036

and cooling condition. The obtained results explain the observed increase in life-time to 200 and 140% during turning and milling, respectively, if the Ti–Al–N coated inserts are annealed at 900 °C.

2. Experimental details

2.1. Coating deposition

Ti–Al–N coatings were deposited onto powder metallurgically prepared CNMG120408 style cemented carbide (WC — 6 wt % Co) and SEET12T3 style cemented carbide (WC — 10 wt% Co) by a commercial cathodic arc evaporation system (Balzers Oerlikon Rapid Cooling System, RCS). Two cathodes are equipped with Ti targets (99.99% purity) for the deposition of a ~30 nm thin TiN interlayer, and four cathodes are equipped with $Ti_{0.34}Al_{0.66}$ targets for preparation of the coating with a thickness of ~3 µm. Prior to the deposition with a two fold substrate-rotation fixture in N_2 (99.99% purity) atmosphere at ~1 Pa, −100 V DC substrate bias and 550 °C, the substrates were cleaned by an Argon-ion-etching process.

2.2. Isothermal annealing

Isothermal annealing of the coated samples has been performed in a vacuum furnace (COD533R) at 0.1 mPa. Heated from room temperature with a heating rate of (RT) 5 K/min, each sample was annealed at 700, 900, and 1100 °C for 2 h using three different furnace cooling conditions (cooling #1–3). In addition, annealing at 900 °C was also conducted for 30 min to investigate the influence of time on the age-hardening behavior. For cooling #1 the heater is switched off after the annealing, resulting in an average cooling rate of ~1 K/min. Cooling #2 is performed in flowing Ar at $9{\cdot}10^4$ Pa pressure, also with the heater switched off resulting in an average cooling rate of ~4 K/min. This is consistent with the cooling treatment of sintered cemented carbide. Cooling #3 is similar to cooling #1, with an overall cooling rate of ~1 K/min in vacuum, but from 800 to 700 °C the temperature is rapidly decreased (~50 K/min) by the help of flowing Ar with $9{\cdot}10^4$ Pa. Fig. 1 shows the schematic patterns of the three cooling conditions. In cemented carbide (WC-Co) alloy with a cobalt content below 20 wt% a phase transition of Co from cubic to hexagonal during cooling is observed in the temperature range 800–700 °C, whereas bulk Co undergoes this phase transition at 417 °C [15].

2.3. Characterization

The chemical composition of the coatings was determined using electron probe microanalysis (EMPA) (JXA-8800R, JEOL) of five regions on each coated sample. The standard deviation for the metal atoms is below 2 at%. Structural investigations are conducted by X-ray diffraction (XRD) with CuKα radiation using a Bruker D8 in Bragg/Brentano mode. The hardness of the coatings is obtained by nano-indentation with 5 mN load using a Fischerscope H100VP after the Oliver and Pharr method [16]. Scratch tests were performed using a scratch tester (MS-T3000 scratch) with a Rockwell C diamond indenter. More details on the characterization experiments are described in Ref. [5].

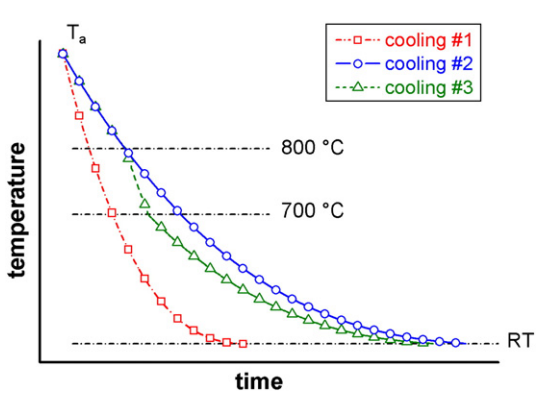

Fig. 1. Schematic patterns of the cooling conditions #1, 2, and 3.

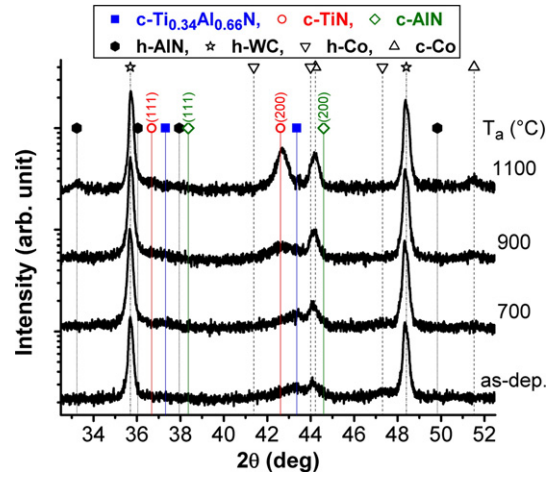

Fig. 2. XRD patterns of $Ti_{0.34}Al_{0.66}N$ coatings in the as-deposited state and after annealing at T_a = 700, 900, and 1100 °C with the cooling condition #1.

The Vickers hardness (HV_{30}) of the cemented carbide substrates in both annealed and un-annealed states were determined with a 270 VRST VM hardens tester under a constant load of 30 kg. The fracture toughness (K_{IC}) was determined through the crack length, which is measured from the tip of the indentation. The thereby estimated K_{IC} belongs to Palmqvist indentation toughness [17] and is calculated after:

$$K_{IC} = 0.15\sqrt{\frac{HV_{30}}{\sum_{i=1}^{4} l_i}}$$

where l_i is the length of the cracks in mm. In order to obtain high accuracy, the specimens were polished with 1 µm diamond paste.

2.4. Cutting tests

Continuous dry turning of stainless steel (1Cr18Ni9Ti) with CNMG120408-EM style inserts (WC — 6 wt% Co) was conducted with a cutting speed (v_c) of 200 m/min, a depth of cut (a_p) of 1.0 mm and a feed rate (f) of 0.2 mm per revolution (mm/r). Dry face milling of steel (42CrMo) with SEET12T3-DM style inserts (WC — 10 wt% Co) was performed with v_c = 320 m/min, a_p = 2.0 mm and f = 0.15 mm/r. The criterion for the tool life-time is when the flank wear lands exceed 0.3 mm.

3. Results and discussion

EPMA measurements show that the nitride coatings are stoichiometric with a chemical composition of $Ti_{0.34}Al_{0.66}N$. Hence, the Ti/Al ratio in the coating corresponds to that of the targets. The surface color of the coatings in as-deposited and annealed states is black for annealing temperatures (T_a) up to 900 °C, and turns into yellow for T_a = 1100 °C.

Fig. 2 shows the XRD patterns of as-deposited $Ti_{0.34}Al_{0.66}N$ coatings and after annealing at 700, 900, and 1100 °C with the cooling condition #1. With increasing T_a to 900 °C, increasing reflexes for c-TiN and c-AlN can be detected indicating spinodal decomposition of the supersaturated $Ti_{0.34}Al_{0.66}N$ phase. This is in agreement to Refs. [6,7]. For T_a = 1100 °C the $Ti_{0.34}Al_{0.66}N$ coating matrix almost completely transformed into c-TiN and the c-AlN transformed into its stable hexagonal form (h-AlN, wurtzite ZnS structure), see Fig. 2. Consequently, the decomposition of our $Ti_{0.34}Al_{0.66}N$ coating into the

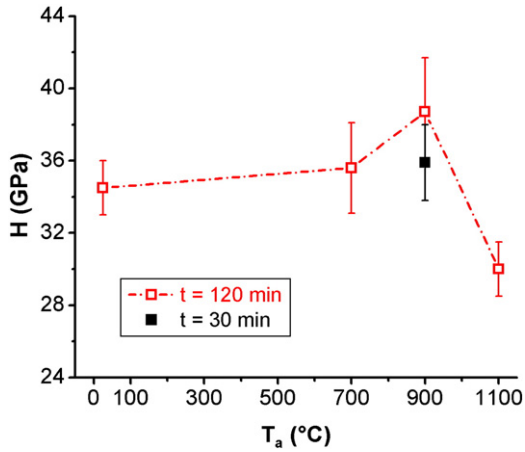

Fig. 3. Hardness of $Ti_{0.34}Al_{0.66}N$ as a function of the annealing temperature T_a using cooling condition #1.

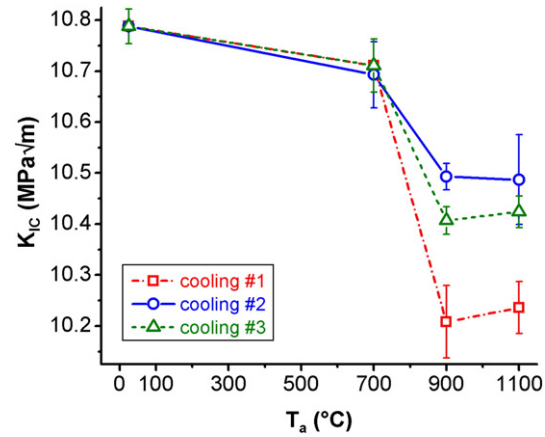

Fig. 5. Fracture toughness of the cemented carbide (WC — 10 wt% Co) substrate in the sintering state and after annealing at T_a=700, 900, and 1100 °C for the cooling conditions #1, 2, and 3.

stable phases c-TiN and h-AlN involves an intermediate step of c-AlN. The formation of stable h-AlN needs a higher driving force than c-AlN due to the nucleation barrier by a different structure to the matrix and a specific volume mismatch of ~26% [6–8]. With increasing annealing temperature, increasing intensity of the c-Co XRD reflexes (at ~44.2 and 51.5 deg) can be detected indicating out-diffusion of Co from the cemented carbide substrate. Additionally the reflexes for h-Co from the surface near region of the cemented carbide substrate decrease in intensity, see Fig. 2.

The hardness (H) of our coatings as a function of annealing temperature and time is presented in Fig. 3. Only a small increase in H from 34.5 to 35.6 GPa is obtained for increasing T_a to 700 °C, which is the initial stage of spinodal decomposition, compare Fig. 3. A maximum in hardness of ~38.7 GPa is obtained after annealing at T_a=900 °C for 120 min due to the formation of coherent c-TiN and c-AlN nm-sized domains [6]. Strain fields, originating from the lattice mismatch between remaining c-Ti–Al–N matrix, c-TiN and c-AlN, act as additional obstacles for the dislocation movement and cause a hardness increase. The transformation of c-AlN into h-AlN and the out-diffusion of Co leads to a drop in hardness to ~30.0 GPa for a further increase in temperature to T_a=1100 °C, see Fig. 3. Hence, our results are in agreement to previous studies [6,8,14]. If the annealing at 900 °C is only conducted for 30 min the hardness only increases to ~35.9 GPa from the as-deposited value of 34.5 GPa. This comparison indicates that the hardness increase of Ti–Al–N coatings due to the formation of c-TiN and c-AlN domains requires sufficient thermal activation and time. Temperature and time influence the degree of transformation and hence the size and amount of obstacles for plastic deformation [18].

The adhesion strength between coating and substrate is characterized by the scratch test at the coating fracture initiation. This force in the as-deposited state and after annealing at 700, 900, and 1100 °C for the different cooling conditions #1–3 is presented in Fig. 4. The adhesive strength almost linearly decreases from the as-deposited value of 78 to 36 N with increasing T_a to 1100 °C, if the fastest cooling rate (cooling #2) is used. This is mainly attributed to the differences in thermal expansion coefficient between substrate and coating. After annealing at T_a=1100 °C the coating near the cutting edge is slightly peeled off from the substrate due to the residual stresses by the rapid cooling and the formation of h-AlN at 1100 °C with the thereby connected volume expansion. The cooling conditions #1 and 3 cause a smaller reduction in adhesive strength with increasing T_a. After

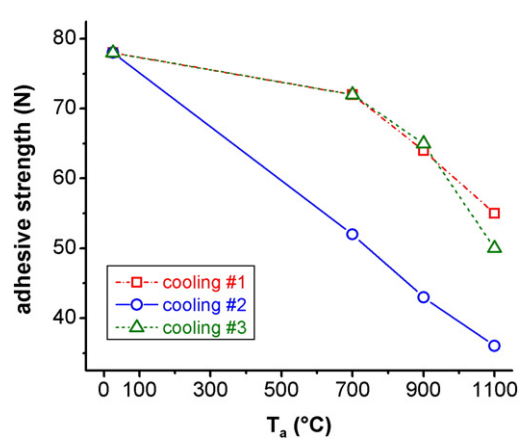

Fig. 4. Scratch test force at the coating fracture initiation (adhesive strength) of the $Ti_{0.34}Al_{0.66}N$ coating on the cemented carbide (WC — 10 wt% Co) in the as-deposited state and after annealing at T_a=700, 900, and 1100 °C for the cooling conditions #1, 2, and 3.

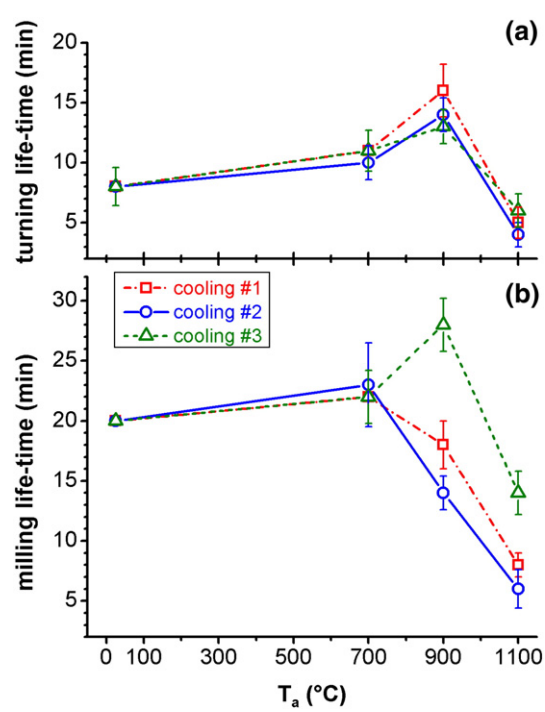

Fig. 6. Life-time of $Ti_{0.34}Al_{0.66}N$ coated inserts during continuous turning of stainless steel (1Cr18Ni9Ti) (a) and milling of 42CrMo steel (b).

annealing at T_a=900 °C, the adhesive strength of the coating on the cemented carbide is still ~65 N for both cooling conditions.

The hardness values of the substrates are constant at ~1710 HV_{30} (WC — 6 wt% Co) and 1630 HV_{30} (WC — 10 wt% Co) independent of the annealing temperature and cooling conditions. Fig. 5 shows the fracture toughness of the (WC — 10 wt% Co) substrate used for milling tools as a function of T_a for different cooling conditions. In general, the fracture toughness of the cemented carbide increases with the Co content. Additionally, the fracture toughness at a given Co content can be optimized by preventing the cubic to hexagonal phase transition of Co during cooling. Consequently, the cooling conditions are essential for the fracture toughness of the cemented carbide. Up to an annealing temperature of 700 °C, the fracture toughness of our substrate (WC — 10 wt% Co) is only slightly reduced from the initial value of ~10.8 to ~10.7 MPa√m, almost independent of the used cooling condition. After annealing at T_a=900 °C, the fracture toughness is reduced to ~10.5, ~10.4 and ~10.2 MPa√m for the cooling conditions #2, 3, and 1, respectively. Hence, the reduction is lower for higher cooling rates. This can be attributed to a decreasing tendency of the Co binder phase transformation from cubic to hexagonal with increasing cooling rate. After annealing at T_a=1100 °C the fracture toughness values are similar to the values after T_a=900 °C, see Fig. 5. The lower Co-containing substrate (WC — 6 wt% Co) shows a similar dependence of the fracture toughness with T_a. Starting from ~9.5 MPa√m the K_{IC} value is reduced to ~9.2 MPa√m by the annealing at T_a=900 °C combined with cooling #1. Consequently, the reduction in K_{IC} by the annealing treatment at 900 °C is more pronounced as for the higher Co-containing substrate.

Regardless of the used cooling condition after annealing at T_a=700 °C, the tool life-time is higher for continuous turning of stainless steel (1Cr18Ni9Ti), see Fig. 6a and milling of 42CrMo steel, see Fig. 6b, compared to the untreated $Ti_{0.34}Al_{0.66}N$ coated inserts. As for continuous turning, the tool life is mainly controlled by the hardness of the coating [17], the longest life-time is obtained after annealing at 900 °C, where the coating hardness is maximum with 38.7 GPa. Here, an increase to 200% of the life-time of untreated inserts is obtained with the slowest cooling rate, as thereby the generated thermal stress is minimal. An increase in tool life-time to ~170% is obtained for the other cooling conditions. For milling, the tool life-time after annealing at T_a=900 °C strongly depends on the used cooling conditions. An increase to 140% of the untreated tool life-time only is obtained by cooling #3, as here the coating has a high adhesive strength of ~65 N to the insert combined with a high fracture toughness of ~10.4 MPa√m of the cemented carbide, compare Figs. 4 and 5. For cooling #1 and 2, the life-time is even reduced to ~90 and 70% as here either the fracture toughness of the cemented carbide is smallest or the adhesive strength, respectively. This is because during milling (i.e. interrupted cutting) the fracture toughness and adhesion of the coating play a more important role than during continuous turning, where mainly the hardness in addition to oxidation determines the overall performance.

4. Conclusions

In this work, we have investigated the industrial application of age-hardening of $Ti_{0.34}Al_{0.66}N$ coatings. Annealing of supersaturated $Ti_{0.34}Al_{0.66}N$ coating at 900 °C results in a hardness increase from 34.5 to 38.7 GPa due to the formation of nm-sized metastable cubic TiN and cubic AlN domains in cubic Ti–Al–N matrix. The life-time of coated inserts during turning of stainless steel is increased to 200% by post-deposition vacuum annealing at 900 °C combined with a ~1 K/min vacuum furnace cooling. During milling of 42CrMo steel an increase in life-time to 140% is only obtained if the cooling after annealing at 900 °C is performed in three steps. The temperature is decreased from 900 to 800 °C by a ~1 K/min vacuum furnace cooling, from 800 to 700 °C by a ~50 K/min Ar-flow cooling, and further to RT again by a ~1 K/min vacuum furnace cooling. This cooling condition allows the combination of an age-hardened coating with a retained high adhesion and high fracture toughness of the cemented carbide. Due to the rapid cooling between 800 and 700 °C the phase transformation of the Co-binder from cubic to hexagonal, occurring in this temperature range, can be retarded. Consequently, the fracture toughness of the coated insert is only reduced from 10.8 to 10.5 MPa√m. The overall slow cooling condition can minimize the thermal stresses due to the mismatch in thermal expansion coefficient between coating and substrate and hence the coating still has a high adhesive strength of ~65 N to the insert.

Based on our results we can conclude that the turning and milling performance of coated inserts can be optimized by a post-deposition annealing treatment, where the coating undergoes age-hardening, combined with a cooling condition allowing for high adhesion and fracture toughness of the cemented carbide. The latter are essential during milling.

Acknowledgements

The financial supports from National Outstanding Youth Science Foundation of China (Grant No. 50425103) and the START Program (project 1371-N14) of the Austrian Science Fund (FWF) are greatly acknowledged. Li Chen thanks the Ministry of Education of China for over-sea student fellowship (Grant No.[2007]3020). Yong Du acknowledges Chang Jiang Scholar Program released by Ministry of Education of China.

References

[1] S. PalDey, S.C. Deevi, Mater. Sci. Eng., A 342 (2003) 58.
[2] K. Kutschej, P.H. Mayrhofer, M. Kathrein, P. Polcik, C. Mitterer, Surf. Coat. Technol. 188–189 (2004) 358.
[3] J.S. Koehler, Phys. Rev., B. 2 (1970) 547.
[4] A.A. Minevich, Surf. Coat. Technol. 53 (1992) 161.
[5] L. Chen, Y. Du, S.Q. Wang, J. Li, Int. J. Refract. Met. Hard Mater. 25 (2007) 400.
[6] P.H. Mayrhofer, A. Hörling, L. Karlsson, J. Sjölen, T. Larsson, C. Mitterer, L. Hultman, Appl. Phys. Lett. 83 (2003) 2049.
[7] P.H. Mayrhofer, L. Hultman, J.M. Schneider, P. Staron, H. Clemens, Int. J. Mater. Res. 98 (2007) 1054.
[8] A. Hörling, L. Hultman, M. Oden, J. Sjölen, L. Karlsson, J. Vac. Sci. Technol. 20 (2002) 1815.
[9] J.W. Cahn, Acta Metall. 9 (1961) 795.
[10] A. Hörling, L. Hultman, M. Oden, J. Sjölen, L. Karlsson, Surf. Coat. Technol. 191 (2005) 384.
[11] K.–D. Bouzakis, N. Michanilidis, S. Hadjiyiannis, E. Pavlidou, G. Erkens, Surf. Coat. Technol. 146–147 (2001) 436.
[12] K.–D. Bouzakis, G. Skordaris, S. Hadjiyiannis, I. Mirisidis, N. Michanilidis, G. Erkens, I. Wirth, Surf. Coat. Technol. 200 (2006) 4500.
[13] G.S. Fox-Rabinovich, J.L. Endrino, B.D. Beake, A.I. Kovalev, S.C. Velduis, L. Ning, F. Fontaine, A. Gray, Surf. Coat. Technol. 201 (2006) 3524.
[14] G.S. Fox-Rabinovich, J.L. Endrino, B.D. Beake, M.H. Aguirre, S.C. Veldhuis, D.T. Quinto, C.E. Bauer, A.I. Kovalev, A. Gray, Surf. Coat. Technol. 202 (2008) 2985.
[15] G.S. Upadhyaya, Mater. Des. 22 (2001) 483.
[16] W.C. Oliver, G.M. Pharr, J. Mater. Res. 7 (1992) 1564.
[17] W.D. Schubert, H. Neumeister, G. Kinger, B. Lux, Int. J. Refract. Met. Hard Mater. 16 (1998) 133.
[18] P.H. Mayrhofer, F.D. Fischer, H.J. Böhm, C. Mitterer, J.M. Schneider, Acta Mater. 55 (2007) 1441.